(12) LEVEL III

AD A089197

AD A082830

RADC-TR-80-219
Interim Report
June 1980

ANALYSIS OF ADVANCED CI APPLICATIONS AND SYSTEMS PERFORMANCE

The Optical Sciences Company

Sponsored by
Defense Advanced Research Projects Agency (DoD)
ARPA Order No. 2646

DTIC
ELECTE
SEP 15 1980
S D
B

APPROVED FOR PUBLIC RELEASE; DISTRIBUTION UNLIMITED

The views and conclusions contained in this document are those of the authors and should not be interpreted as necessarily representing the official policies, either expressed or implied, of the Defnese Advanced Research Projects Agency or the U.S. Government

ROME AIR DEVELOPMENT CENTER
Air Force Systems Command
Griffiss Air Force Base, New York 13441

DDC FILE COPY

80 9 15 105

This report has been reviewed by the RADC Public Affairs Office (PA) and is releasable to the National Technical Information Service (NTIS). At NTIS it will be releasable to the general public, including foreign nations.

RADC-TR-80-219 has been reviewed and is approved for publication.

APPROVED: Donald W. Hanson

DONALD W. HANSON
Project Engineer

Include this notice with any reproduced portion of this document.

If your address has changed or if you wish to be removed from the RADC mailing list, or if the addressee is no longer employed by your organization, please notify RADC (OCSE) Griffiss AFB NY 13441. This will assist us in maintaining a current mailing list.

Do not return this copy. Retain or destroy.

MISSION
of
Rome Air Development Center

RADC plans and executes research, development, test and selected acquisition programs in support of Command, Control Communications and Intelligence (C^3I) activities. Technical and engineering support within areas of technical competence is provided to ESD Program Offices (POs) and other ESD elements. The principal technical mission areas are communications, electromagnetic guidance and control, surveillance of ground and aerospace objects, intelligence data collection and handling, information system technology, ionospheric propagation, solid state sciences, microwave physics and electronic reliability, maintainability and compatibility.

ANALYSIS OF ADVANCED CI APPLICATIONS AND SYSTEMS PERFORMANCE

David L. Fried

Contractor: The Optical Sciences Company
Contract Number: F30602-79-C-0062
Effective Date of Contract: 20 March 1979
Contract Expiration Date: 30 September 1980
Short Title of Work: Analysis of Advanced CI
Program Code Number: 0E20
Period of Work Covered: October 1979 - March 1980
Principal Investigator: Dr. David L. Fried
Phone: 714-524-3622

Project Engineer: Donald W. Hanson
Phone: 315-330-3145

Approved for public release; distribution unlimited

This research was supported by the Defense Advanced Research Projects Agency of the Department of Defense and was monitored by Donald W. Hanson (OCSE), Griffiss AFB NY 13441 under Contract F30602-79-C-0062.

DTIC
ELECTE
SEP 15 1980
B

UNCLASSIFIED

SECURITY CLASSIFICATION OF THIS PAGE (When Data Entered)

REPORT DOCUMENTATION PAGE

READ INSTRUCTIONS BEFORE COMPLETING FORM

1. REPORT NUMBER: RADC-TR-80-219
2. GOVT ACCESSION NO.: AD-A089197
3. RECIPIENT'S CATALOG NUMBER:
4. TITLE (and Subtitle): ANALYSIS OF ADVANCED CI APPLICATIONS AND SYSTEMS PERFORMANCE
5. TYPE OF REPORT & PERIOD COVERED: Interim Report Oct 1979 — Mar 1980
6. PERFORMING ORG. REPORT NUMBER: DR-169
7. AUTHOR(s): David L. Fried
8. CONTRACT OR GRANT NUMBER(s): F30602-79-C-0062 ARPA Order-2646
9. PERFORMING ORGANIZATION NAME AND ADDRESS: The Optical Sciences Company, PO Box 446, Placentia CA 92670
10. PROGRAM ELEMENT, PROJECT, TASK AREA & WORK UNIT NUMBERS: 26460411, 62301E
11. CONTROLLING OFFICE NAME AND ADDRESS: Defense Advanced Research Projects Agency, 1400 Wilson Blvd, Arlington VA 22209
12. REPORT DATE: June 1980
13. NUMBER OF PAGES: 58
14. MONITORING AGENCY NAME & ADDRESS (if different from Controlling Office): Rome Air Development Center (OCSE), Griffiss AFB NY 13441
15. SECURITY CLASS. (of this report): UNCLASSIFIED
15a. DECLASSIFICATION/DOWNGRADING SCHEDULE: N/A
16. DISTRIBUTION STATEMENT (of this Report): Approved for public release; distribution unlimited
17. DISTRIBUTION STATEMENT (of the abstract entered in Block 20, if different from Report): Same
18. SUPPLEMENTARY NOTES: RADC Project Engineer: Donald W. Hanson (OCSE)
19. KEY WORDS (Continue on reverse side if necessary and identify by block number)

Atmospheric Optics	Antenna Gain
Turbulence	Ambiguity
Adaptive Optics	Deformable Mirror
Speckle Interferometry	

20. ABSTRACT (Continue on reverse side if necessary and identify by block number)

In this report three problems associated with compensated imaging and adaptive optics are considered. Chapter 1 is concerned with the matter of the effect of turbulence induced intensity variations at an aperture upon the antenna gain achievable when the aperture is used as a laser transmitter. Chapter 2 treats a problem related to image recovery from speckle interferometry data - namely the question of ambiguity in the result when the image recovery is based on nonnegativity of intensity.

DD FORM 1 JAN 73 1473 EDITION OF 1 NOV 65 IS OBSOLETE

UNCLASSIFIED

SECURITY CLASSIFICATION OF THIS PAGE (When Data Entered)

391358

Chapter 3 examines a concept for producing low voltage multielement adaptive optics deformable mirrors.

The effect on average antenna gain of the inability of an adaptive optics laser transmitter to vary the intensity of the laser beam across the transmitter aperture is evaluated. In Chapter 1 this is found to result in a degradation of the average antenna gain by a factor of $\exp(-\sigma_\ell^2)$, where σ_ℓ^2 is the log-amplitude variance of the received beacon signal. It is shown there that if the adaptive optics can accommodate the need to be able to vary the laser intensity across the transmitter's aperture, then the average antenna gain can be made to equal the diffraction limited antenna gain. This is achieved when the adaptive optics implements wave function conjugation, transmitting a low/high laser intensity from those points in the transmitter aperture where the received beacon signal is correspondingly low/high.

In Chapter 2 the question of whether the constraint that no part of an image can be negative is sufficient to insure unambiguous reconstruction of an image from its power spectrum is studied. The question is relevant to the problem of whether or not the Labeyrie technique is sufficient to allow image extraction from speckle data. It is shown there that a whole class of images exists for which extensive ambiguity is present in the process of extracting the image from its power spectrum (or rather from its correlation function). In the absence of any reason to consider members of this class of images inherently uninteresting, it is suggested that a technique like the Knox-Thompson algorithm be preferred to the Labeyrie technique with nonnegativity for image extraction from speckle data.

The need for a low voltage multielement deformable mirror is well known. In Chapter 3 a concept is developed for just such a piezoelectrically activated deformable mirror. The concept is based on use of the d_{31} piezoelectric coefficient, forming a piezoelectric "block" from a set of long narrow rods. Assembly techniques are suggested. Supporting performance analysis is developed.

PREFACE

This report is submitted in accordance with the requirements of Contract No. F30602-79-C-0062. It represents the results of work completed between October 1979 and March 1980.

This report is a collection of several reports which previously had been issued only informally. They are assembled in this document, each constituting a single chapter.

ACCESSION for	
NTIS	White Section ☑
DDC	Buff Section ☐
UNANNOUNCED	☐
JUSTIFICATION	
BY	
DISTRIBUTION/AVAILABILITY CODES	
Dist. AVAIL. and/or SPECIAL	
A	

TABLE OF CONTENTS

LIST OF FIGURES

Chapter 1

Laser Transmitter Adaptive Optics Compensation

for

Intensity Variations on the Aperture

1.1 Introduction

The theoretical basis for a phase conjugation adaptive optics laser transmitter is found in the reciprocity theorem proved by Lutomirski and Yura in an appendix of their paper[1]. They prove that the wave function $U(\vec{R}_1, \vec{R}_2)$ for propagation from a point source at $\vec{R}_1$ to a measurement point at $\vec{R}_2$ is identical to the wave function $U(\vec{R}_2, \vec{R}_1)$ associated with propagation from a point source at $\vec{R}_2$ to a measurement point at $\vec{R}_1$.

$$U(\vec{R}_1, \vec{R}_2) = U(\vec{R}_2, \vec{R}_1) \quad . \tag{1}$$

This result follows from the time reversal invariance of Maxwell's equations, and applies for any propagation medium (except for certain magneto-optically active materials). From this it follows in a very direct way that if the effect of a random medium is to introduce only phase variations in $U(\vec{R}_1, \vec{R}_2)$, then to transmit to $\vec{R}_1$ with an antenna gain that is undegraded by the propagation medium, the wave that is launched by the transmitter should correspond to the complex conjugate of the wave received from $\vec{R}_1$, i.e., that the transmitted wave should be proportional to $U^*(\vec{R}_1, \vec{R}_2)$.

The proof of this result is so straightforward that, to the best of our knowledge, no proof has ever been published. This result, however, assumes, as noted above, that the effect of any irregularities in the propagation medium affects only the phase of $U(\vec{R}_1, \vec{R}_2)$, and has no affect on the amplitude of $U(\vec{R}_1, \vec{R}_2)$. In this work, however, we shall be concerned with the effect of such amplitude variations on antenna gain if the adaptive optics only makes phase corrections, and with the question of what we would like the adaptive optics to do to the amplitude of the transmitted wave to maximize antenna gain—assuming that the adaptive optics could produce any desired variation of the amplitude of the transmitted wave without having to "throw away" transmitter power. For example, should the amplitude of the transmitted wavefront be large where the amplitude of $U(\vec{R}_1, \vec{R}_2)$ is small so as

in effect to compensate for it, or should it also be small, as would be suggested by the "principle" of transmitting the conjugate wavefront, $U^*(\vec{R}_1, \vec{R}_2)$. We shall show that this later is, in fact, the correct strategy for maximizing antenna gain.

We shall restrict our analysis to the case of propagation through atmospheric turbulence. We shall utilize various well known[2] results associated with the theory of propagation through turbulence. In particular, we utilize the fact that the logarithm of the turbulence induced amplitude variations follows a gaussian distribution, and that such log-amplitude variations manifest a rather short correlation range. We shall also restrict our attention to an adaptive optics control logic which calculates the log-amplitude of the transmitted wave as a linear function of the log-amplitude of the received beacon signal at the same point on the transmitter aperture.

In the next section we shall consider the situation when the adaptive optics provide for no variation of the intensity of the transmitted beam across the transmitter aperture. This will provide a definitive result for the extent of the loss in transmitter antenna gain due to completely uncompensated intensity effects across the aperture. There it will be shown that the effect is to reduce the antenna gain by a factor of $\exp(-\sigma_\ell^2)$, where σ_ℓ^2 is the log-amplitude variance. The section after that will consider the dependence of transmitter antenna gain on the form of the compensation of intensity across the transmitter aperture. It will be shown that transmitter antenna gain is optimized by making the variations across the aperture of the intensity of the transmitted wave exactly match (i.e., directly proportional to) the variations across the aperture of intensity of the received beacon signal. It will be seen that with just such variations of intensity of the transmitted beam, the average transmitter antenna gain will be just what would have been achieved in the absence of turbulence effects.

1.2 Antenna Gain With No Intensity Pattern Compensation

For the purposes of the analysis we shall be carrying out here, it will be convenient to represent the turbulence corrupted wave as received from a point source beacon colocated with the target aimpoint of our adaptive optics by the notation

$$U(\vec{R}, \vec{r}) = u(\vec{R}, \vec{r})\, W(\vec{r})\, \exp[\chi(\vec{r}) + i\,\phi(\vec{r})] \quad , \tag{2}$$

where $\vec{r}$ is a two dimensional vector denoting position on the plane of the transmitter aperture, and $\vec{R}$ is a vector denoting the position of the point source beacon. ($\vec{R}$ is also the position of the aimpoint of the laser transmitter.) The function $u(\vec{R}, \vec{r})$ represents the wave function from the beacon to the transmitter aperture in the absence of turbulence effects, while the function $W(\vec{r})$ defines the extent of the transmitter aperture in accordance with the equation

$$W(\vec{r}) = \begin{cases} 1, & \text{if } \vec{r} \text{ represents a point within the aperture,} \\ 0, & \text{if } \vec{r} \text{ represents a point outside of the aperture.} \end{cases} \tag{3}$$

The function $\phi(\vec{r})$ denotes the ordinary, i.e., the phase portion of the turbulence induced wavefront distortion while the function $\chi(\vec{r})$ denotes the natural logarithm of the turbulence induced variation of the amplitude of the beacon signal.

In accordance with well established results of propagation theory[2] we can consider both $\phi(\vec{r})$ and $\chi(\vec{r})$ to be gaussian random functions, though it is only the properties of $\chi(\vec{r})$, the log-amplitude variation, that will be of concern to us in this paper. Moreover, it is well established that the statistics of these random functions are homogeneous and isotropic. The statistics of the log-amplitude variation are characterized by a mean value, $\overline{\chi}$, where

$$\overline{\ell} = \langle \ell(\vec{r}) \rangle \quad , \tag{4}$$

and a covariance function, $C_\ell(\rho)$, where

$$C_\ell(\rho) = \langle [\ell(\vec{r}) - \overline{\ell}] [\ell(\vec{r}') - \overline{\ell}] \rangle \quad , \tag{5}$$

with

$$\rho = |\vec{r} - \vec{r}'| \quad . \tag{6}$$

For convenience we also define the log-amplitude variance, σ_ℓ^2, as

$$\sigma_\ell^2 = C_\ell(0) \quad . \tag{7}$$

It can be shown[3] that by virtue of conservation of energy considerations it is necessary that

$$\overline{\ell} = -\sigma_\ell^2 \quad . \tag{8}$$

This relationship is required since positive and negative values of $\ell(\vec{r})$ do not change the power density by the same amount. The bias in the distribution provided by having $\overline{\ell}$ not equal to zero is necessary so that equal but opposite sign values of $\ell(\vec{r})$ will not occur with equal probability. The value of $\overline{\ell}$ specified by Eq. (8) provides exactly the required bias of the probability distribution.

If the laser transmitter emits a wave function $\psi(\vec{r})$, then it can be shown that the power density at the beacon/aimpoint will be

$$\rho = \tfrac{1}{2} \left| \frac{-i}{\lambda \mathcal{L}} \int d\vec{r}\, U(\vec{R}, \vec{r})\, \psi(\vec{r}) \right|^2 \quad , \tag{9}$$

where in writing this formula we have made use of the reciprocity result of Lutomirski and Yura as embodied in Eq. (1) to introduce the effect of propagation from each point in the aperture, through the turbulent atmosphere, to the aimpoint. The range of integration in Eq. (9) is to be understood as being limited to the transmitter aperture by virtue of the fact that $\mathcal{V}(\vec{r})$ vanishes for values of $\vec{r}$ outside the aperture. In Eq. (9) the quantity $\mathcal{R}$ denotes the range from the transmitter to the aimpoint. The antenna gain, G, may be considered to be equal to the ratio of power density at the aimpoint to the total transmitter power, scaled as range squared. Thus, we can write

$$G = \frac{\mathcal{R}^2}{\int d\vec{r}\, \frac{1}{2} |\mathcal{V}(\vec{r})|^2} \quad . \tag{10}$$

Combining Eq.'s (9) and (10), we can write for the laser transmitter antenna gain

$$G = \frac{\lambda^{-2} \left| \int d\vec{r}\, U(\vec{R}, \vec{r})\, \mathcal{V}(\vec{r}) \right|^2}{\int d\vec{r}\, |\mathcal{V}(\vec{r})|^2} \quad . \tag{11}$$

At this point it is convenient to take up consideration of the very simple case in which there are no turbulence effects.

When there are no turbulence effects present the wave function $U(\vec{R}, \vec{r})$, as defined by Eq. (2), reduces to the very simple form

$$U_o(\vec{R}, \vec{r}) = u(\vec{R}, \vec{r})\, W(\vec{r}) \quad . \tag{12}$$

The function $u(\vec{R}, \vec{r})$ can be considered to be a constant amplitude function (providing that the beacon source is not so large that it can be resolved by the transmitter's aperture) with only a phase dependence, $\phi(\vec{r})$, across the transmitter aperture. Accordingly, we can write

$$u(\vec{R},\vec{r}) = \exp[i\,\psi(\vec{r})] \quad . \tag{13}$$

Making use of Eq.'s (12) and (13) in conjunction with Eq. (11), the antenna gain, in the absence of turbulence, can be written as

$$G_o = \lambda^{-2}\,\frac{\left|\int d\vec{r}\; W(\vec{r})\,\exp[i\,\psi(\vec{r})]\,\gamma(\vec{r})\right|^2}{\int d\vec{r}\;|\gamma(\vec{r})|^2} \quad . \tag{14}$$

With a laser wave function of uniform amplitude $\mathcal{A}$ leaving the transmitter aperture, the turbulence free antenna gain, G_o, will be maximized when the laser wave function has the form

$$\gamma_o(\vec{r}) = \mathcal{A}\,\exp[-i\,\psi(\vec{r})]\,W(\vec{r}) \quad . \tag{15}$$

This exactly corresponds to focusing the transmitted wavefront on the target, and in this case we get

$$G_o = \lambda^{-2}\,\frac{\left|\int d\vec{r}\; W(\vec{r})\right|^2}{\int d\vec{r}\; W(\vec{r})} \quad . \tag{16}$$

If we let A denote the transmitter aperture area, i.e.,

$$A = \int d\vec{r}\; W(\vec{r}) \quad , \tag{17}$$

then we can write

$$G_o = A/\lambda^2 \quad , \tag{18}$$

and for the special case of a clear circular aperture of diameter D we get

$$G_o = \tfrac{1}{4}\,\pi\,(D/\lambda)^2 \quad . \tag{19}$$

When turbulence is present the beacon signal will have the form

$$U(\vec{R},\vec{r}) = \exp[i\,\psi(\vec{r})]\,W(\vec{r})\,\exp[\ell(\vec{r}) + i\,\phi(\vec{r})] \quad , \tag{20}$$

which is obtained by substituting Eq. (13) into Eq. (2). In this case, by combining Eq.'s (11) and (20) we see that the antenna gain is expressible as.

$$G = \lambda^{-2}\,\frac{\left|\int d\vec{r}\; W(\vec{r})\,\exp[i\,\psi(\vec{r})]\exp[\ell(\vec{r}) + i\phi(\vec{r})]\gamma(\vec{r})\right|^2}{\int d\vec{r}\;\left|\gamma(\vec{r})\right|^2} \quad . \tag{21}$$

Since, for this section, we are restricting our attention to the case in which the adaptive optics in the laser transmitter will only distort the wavefront shape of $\gamma(\vec{r})$ but will leave the amplitude of $\gamma(\vec{r})$ unchanged, i.e., independent of $\vec{r}$, it is obvious from consideration of Eq. (21) that the distorted wavefront will have a phase that exactly compensates for $\psi(\vec{r})$ and $\phi(\vec{r})$. This will insure that the integrand in the integral in the numerator in Eq. (21) will be everywhere positive, which choice maximizes the value of that integral. The adaptive optics would cause the laser wavefront to be represented by the expression

$$\gamma(\vec{r}) = \mathcal{A}\exp[-\,i\,\psi(\vec{r}) - i\,\phi(\vec{r})]\,W(\vec{r}) \quad . \tag{22}$$

The $\psi(\vec{r})$-dependence in Eq. (22) is just that which [as in the turbulence free case corresponding to Eq. (15)] is required to focus the beam on the aimpoint taking appropriate account of the various geometric factors. The $\phi(\vec{r})$-dependence in Eq. (22) corresponds to correction for the phase shift portion of the turbulence effect, and in a limited sense corresponds to phase conjugation correction of turbulence effects.

When Eq. (22) is substituted into Eq. (21), we get the result that

$$G = \lambda^{-2} \frac{\left|\int d\vec{r}\, W(\vec{r}) \exp[\ell(\vec{r})]\right|^2}{\int d\vec{r}\, W(\vec{r})} \quad . \tag{23}$$

In as much as the log-amplitude variation, $\ell(\vec{r})$, is a random function it is obvious that the antenna gain, G, as specified by Eq. (23), is a random variable. Our interest is actually in the average value of the antenna gain, which we can write as

$$\langle G \rangle = \lambda^{-2} \frac{\langle \{\int d\vec{r}\, W(\vec{r}) \exp[\ell(\vec{r})]\}^2 \rangle}{\int d\vec{r}\, W(\vec{r})} \quad . \tag{24}$$

In developing Eq. (24) from Eq. (23) we have made use of the fact that the integrand for this integral in the numerator is everywhere real and positive, so that the value of that integral must also be real and positive. This allowed us to drop the absolute value bars.

By writing the square of an integral as the product of two integrals (one taken over the variable $\vec{r}$, and the other taken over the variable $\vec{r}'$), then writing the product of two integrals as a double integral, and finally, interchanging the order of integration and ensemble averaging, we can obtain the result that

$$\langle \{\int d\vec{r}\, W(\vec{r}) \exp[\ell(\vec{r})]\}^2 \rangle$$

$$= \iint d\vec{r}\, d\vec{r}'\, W(\vec{r})\, W(\vec{r}') \langle \exp[\ell(\vec{r}) + \ell(\vec{r}')] \rangle \quad . \tag{25}$$

To evaluate the ensemble average term on the right-hand-side of Eq. (25) we make use of the fact that if χ is a zero mean gaussian random variable and a is any constant, then it can be shown that[4]

$$\langle \exp(a\chi) \rangle = \exp(\tfrac{1}{2} a^2 \langle \chi^2 \rangle) \quad . \tag{26}$$

Making use of this result we can write

$$\langle \exp[\ell(\vec{r}) + \ell(\vec{r}')] \rangle = \langle \exp\{[\ell(\vec{r}) - \overline{\ell}] + [\ell(\vec{r}') - \overline{\ell}]\} \rangle \exp(2\overline{\ell})$$

$$= \exp\left(\tfrac{1}{2} \langle \{[\ell(\vec{r}) - \overline{\ell}] + [\ell(\vec{r}') - \overline{\ell}]\}^2 \rangle\right) \exp(2\overline{\ell}) \,. \qquad (27)$$

By means of Eq.'s (5), (7), and (8) this can be reduced to

$$\langle \exp[\ell(\vec{r}) + \ell(\vec{r}')] \rangle = \exp\left(\tfrac{1}{2} \{C_\ell(0) + 2C_\ell(|\vec{r} - \vec{r}'|) + C_\ell(0)\}\right)$$

$$\times \exp(-2\sigma_\ell^2)$$

$$= \exp[C_\ell(|\vec{r} - \vec{r}'|) - \sigma_\ell^2] \,. \qquad (28)$$

When we substitute Eq. (28) into Eq. (25), we obtain the result that

$$\langle \{\int d\vec{r}\, W(\vec{r}) \exp[\ell(\vec{r})]\}^2 \rangle$$

$$= \exp(-\sigma_\ell^2) \iint d\vec{r}\, d\vec{r}'\, W(\vec{r})\, W(\vec{r}') \exp[C_\ell(|\vec{r} - \vec{r}'|)]. \qquad (29)$$

We can form an estimate of the value of the double integral on the right-hand-side of Eq. (29) by noting $C_\ell(|\vec{r} - \vec{r}'|)$ has a value less than σ_ℓ^2, which in general, will be less than[5] 0.25, and that for laser transmitter aperture sizes of practical interest the diameter is so much greater than the correlation length associated with $C_\ell(|\vec{r} - \vec{r}'|)$ that for almost all pairs of values of $\vec{r}$ and $\vec{r}'$ the value of $C_\ell(|\vec{r} - \vec{r}'|)$ is very nearly equal to zero. This suggests that with only a modest effect on the accuracy of our results, we can replace the exponential in the double integral by unity. Once we make this replacement the double integral can be rewritten as the product of two identical integrals, each of which is evaluated in Eq. (17). Thus,

we can write from Eq. (29) that

$$\langle [\int d\vec{r}\, W(\vec{r}) \exp[\ell(\vec{r})]]^2 \rangle \approx A^2 \exp(-\sigma_\ell^2) \quad . \tag{30}$$

When we substitute this result into Eq. (24), and again make use of Eq. (17) we obtain a result which can be reduced to the form

$$\langle G \rangle = (A/\lambda^2) \exp(-\sigma_\ell^2) \quad . \tag{31}$$

Taking note of Eq. (18), and defining the intensity variation (random apodization) reduced efficiency, η_{RA}, of the antenna gain of the phase-only-correcting adaptive optics laser transmitter as the ratio of average antenna gain, $\langle G \rangle$, to the diffraction limited antenna gain, G_o, i.e.,

$$\eta_{RA} = \langle G \rangle / G_o \quad , \tag{32}$$

we see that this efficiency factor is given by the expression

$$\eta_{RA} = \exp(-\sigma_\ell^2) \quad . \tag{33}$$

This expression represents the basic result when the adaptive optics of the laser transmitter take no account of the intensity variations of the beacon signal. The transmitted laser beam is of uniform intensity across the aperture and there is only phase distortion correction.

This probably represents a practical limit. Nonetheless, it is interesting to consider the question of achievable antenna gain when the intensity of the transmitted laser beam across can be adjusted. In the next section we take up the question of what is the optimum form of the intensity adjustment, i.e., how do we determine what intensity pattern to transmit given the intensity pattern of the received beacon signal, and what then is the achieved average antenna gain.

1.3 Antenna Gain With Intensity Pattern Compensation

If the adaptive optics portion of the laser transmitter is able not only to adjust the shape of the laser wavefront leaving the transmitter aperture (i.e., make phase corrections), but is also able to redistribute the laser power so as to provide any desired power density pattern across the transmitter aperture (i.e., make a random apodization correction), then it should be possible to compensate, at least in part, for the intensity effects that gave rise to the less-than-unity value of η_{RA} . In this section, we shall establish the exact form of the desired random apodization and shall show that with an optimized choice of this apodization, we can achieve an average antenna gain equal to the diffraction limited value.

The idea that ideal adaptive optics performance is provided by wave function conjugation carries with it the implication that the power density of the transmitted laser beam should vary across the transmitter aperture in exactly the same way that the power density of the received beacon signal varies across the aperture. Where the intensity of one is high, the intensity of the other should be correspondingly high, and where the one is low, the other should also be similarly low. This is in juxtaposition with the seemingly plausible thought that where the one is high, the other should be low, and vice versa. We shall show that in fact use of the wave function conjugation concept does lead to optimum correction, i.e., that the power density of the transmitted laser beam should match that of the received beacon signal.

With wave function conjugation, the random apodization corrected laser wave function would , in place of the form given in Eq. (22), have the form

$$\psi_{WC}(\vec{r}) = \mathcal{A} \exp\left[-i\,\psi(\vec{r}) + \chi(\vec{r}) - i\phi(\vec{r})\right] W(\vec{r}) \quad . \tag{34}$$

The fact that the exponent depends on plus $\ell(\vec{r})$ rather than on minus $\ell(\vec{r})$ implies that the intensity variations of the laser beam match the intensity variations of the beacon, rather than being the inverse. To allow for the fact that the optimum intensity pattern may be different from that developed by wavefront conjugation, we shall consider transmission of the laser wave function corresponding to the expression

$$\gamma_a(\vec{r}) = \mathcal{A} \exp\left[-i\,\psi(\vec{r}) + \alpha\ell(\vec{r}) - i\phi(\vec{r})\right] W(\vec{r}) \quad , \tag{35}$$

where α is a constant whose value is to be determined based on antenna gain optimization criteria. Our choice of this sort of function is based on the following two considerations. First, the intensity pattern across the aperture of the transmitted laser beam should depend on the intensity of the received beacon signal in a way that is unchanged by such things as a doubling of the beacon intensity everywhere over the aperture. This is satisfied by making the log-amplitude of the transmitted laser beam a linear function of the log-amplitude of the received beacon signal. Second, the intensity of the transmitted laser beam should be a local function of the intensity of the received beacon signal. This means that the log-amplitude of the transmitted laser beam at position $\vec{r}$ should depend on the log-amplitude of the received beacon signal only at position $\vec{r}$. The expression given in Eq. (35) is the most general expression we can write satisfying both of these criteria. Our problem now reduces to developing an expression for the average antenna gain as a function of α , and then determining the value of α that maximizes the average antenna gain. We shall find, when we carry out this analysis, that the optimum antenna gain is in fact achieved when α equals unity. Comparison of Eq.'s (34) and (35) makes it clear that that this fact implies that wave function conjugation does indeed yield the optimum compensation for the random apodization induced by atmospheric turbulence, as well as of course completely correcting for the turbulence-induced phase perturbations. We shall see that with wave function conjugation

the average antenna gain is equal to the diffraction limited antenna gain. In terms of average antenna gain, wave function conjugation completely eliminates the effect of atmospheric turbulence

To develop an expression for the dependence of antenna gain on the value of the parameter α we start with Eq. (10). This expression gives the instantaneous antenna gain as the ratio of the instantaneous "range scaled" power density at the target to the instantaneous total laser power leaving the transmitter aperture. For our purposes it is not really appropriate to take the ensemble average of the instantaneous ratio on the right-hand-side of Eq. (10) and consider that to be the average antenna gain. Rather, we should consider the ratio of the ensemble average of the instantaneous "range scaled" power density at the aimpoint to the ensemble average of the instantaneous total laser power leaving the transmitter aperture as being the effective average antenna gain. It is this ratio, which is denoted by $\overline{G}_a$, which we wish to maximize.

In view of this discussion, and starting with Eq. (10), we can write

$$\overline{G}_a = \frac{\langle \mathcal{P}^2 \rangle}{\langle \int d\vec{r}\, \tfrac{1}{2} |\gamma_a(\vec{r})|^2 \rangle} \quad . \tag{36}$$

Proceeding in exactly the same way that we did in going from Eq. (10) to Eq. (21), we can obtain from Eq. (36) the result that

$$\overline{G}_a = \lambda^{-2} \frac{\langle \left| \int d\vec{r}\, W(\vec{r}) \exp[i\psi(\vec{r})] \exp[\chi(\vec{r}) + i\phi(\vec{r})] \gamma_a(\vec{r}) \right|^2 \rangle}{\langle \int d\vec{r}\, |\gamma_a(\vec{r})|^2 \rangle} \quad . \tag{37}$$

When we substitute Eq. (35) into this equation and appropriately simplify, we obtain the result that

$$\overline{G}_\alpha = \lambda^{-2} \frac{\langle \left| \int d\vec{r}\, W(\vec{r}) \exp[(1+\alpha)\, \ell(\vec{r})] \right|^2 \rangle}{\langle \int d\vec{r}\, W(\vec{r}) \exp[2\alpha\, \ell(\vec{r})] \rangle} \quad . \tag{38}$$

Our problem now is to make manifest the nature of the α-dependence in this expression.

We start by noting that by commuting the operations of integration and ensemble averaging, we can write for the denominator of Eq. (38)

$$\langle \int d\vec{r}\, W(\vec{r}) \exp[2\alpha\, \ell(\vec{r})] \rangle = \int d\vec{r}\, W(\vec{r}) \langle \exp[2\alpha\, \ell(\vec{r})] \rangle \quad . \tag{39}$$

Making use of Eq.'s (5), (7), (8), and (26), we can write

$$\begin{aligned} \langle \exp[2\alpha\, \ell(\vec{r})] \rangle &= \langle \exp\{2\alpha\, [\ell(\vec{r}) - \overline{\ell}]\} \rangle \exp(2\alpha\overline{\ell}) \\ &= \exp(2\,\alpha^2\, \sigma_\ell^2) \exp(2\,\alpha\overline{\ell}) \\ &= \exp(2\,\alpha^2 \sigma_\ell^2) \exp(-2\,\alpha\sigma_\ell^2) \\ &= \exp[2(\alpha^2 - \alpha)\, \sigma_\ell^2] \quad . \end{aligned} \tag{40}$$

When we substitute Eq. (40) into Eq. (39) and make use of Eq. (17), we can obtain the result that

$$\langle \int d\vec{r}\, W(\vec{r}) \exp[2\,\alpha\, \ell(\vec{r})] \rangle = A \exp\left[2(\alpha^2 - \alpha)\, \sigma_\ell^2\right] \quad . \tag{41}$$

This completes our evaluation of the denominator in the right-hand-side of Eq. (38). We now have to evaluate the numerator.

To evaluate the numerator of the right-hand-side of Eq. (38), we shall follow basically the same procedure that we used in proceeding from Eq. (25) to Eq. (30). We start by noting that we can write the square of an

integral* as a product of integrals, and then write the product of integrals as a double integral. In this form we can commute the operations of integration and ensemble averaging. Thus, we obtain the result that

$$\left\langle \left| \int d\vec{r}\, W(\vec{r}) \exp[(1+\alpha)\, \ell(\vec{r})] \right|^2 \right\rangle$$

$$= \iint d\vec{r}\, d\vec{r}'\; W(\vec{r})\, W(\vec{r}') \left\langle \exp[(1+\alpha)\,[\ell(\vec{r}) + \ell(\vec{r}')]] \right\rangle \quad . \quad (42)$$

Again, making use of Eq.'s (5), (7), (8), and (26), we can write

$$\left\langle \exp[(1+\alpha)\,[\ell(\vec{r}) + \ell(\vec{r}')]] \right\rangle$$

$$= \left\langle \exp\Big((1+\alpha)\{[\ell(\vec{r}) - \overline{\ell}] + [\ell(\vec{r}') - \overline{\ell}]\}\Big) \exp[2(1+\alpha)\overline{\ell}] \right.$$

$$= \exp[\tfrac{1}{2}(1+\alpha)^2 [\sigma_\ell^2 + 2C_\ell(|\vec{r} - \vec{r}'|) + \sigma_\ell^2]] \exp[-2(1+\alpha)\sigma_\ell^2]$$

$$= \exp[(\alpha^2 - 1)\sigma_\ell^2] \exp[(1+\alpha)^2\, C_\ell(|\vec{r} - \vec{r}'|)] \quad . \quad (43)$$

Combining Eq.'s (42) and (43) and appropriately simplifying, we get the result that

$$\left\langle \left| \int d\vec{r}\, W(\vec{r}) \exp[(1+\alpha)\, \ell(\vec{r})] \right|^2 \right\rangle = \exp[(\alpha^2 - 1)\, \sigma_\ell^2]$$

$$\times \iint d\vec{r}\, d\vec{r}'\, W(\vec{r}) W(\vec{r}') \exp[(1+\alpha)^2 C_\ell(|\vec{r} - \vec{r}'|)] \quad . \quad (44)$$

Here again, just as in going from Eq. (29) to Eq. (30), we make use of the argument that the correlation range for log-amplitude variations is so small

---

* Since the integrand is everywhere real and positive, the integral is also real and positive. This allows us to simply ignore the presence of the absolute value bars in the numerator of the right-hand-side of Eq. (38).

compared to the telescope aperture diameter that for practically all values of $\vec{r}$ and $\vec{r}'$, $C_\ell(|\vec{r} - \vec{r}'|)$ is nearly equal to zero, and that even for the limited set of cases where $\vec{r}$ and $\vec{r}'$ are close together, the correlation is not particularly large. This allows us to estimate the value of the double integral on the right-hand-side of Eq. (44) by replacing the exponential function by unity. Thus, we obtain the result, making use of Eq. (17), that

$$\langle \left| \int d\vec{r}\, W(\vec{r}) \exp[(1 + \alpha)\, \ell(\vec{r})] \right|^2 \rangle \approx A^2 \exp[(\alpha^2 - 1)\sigma_\ell{}^2] \quad . \qquad (45)$$

With this result in hand we can now evaluate the average antenna gain.

When we substitute Eq.'s (41) and (45) into Eq. (38) and appropriately simplify the result, we get the equation

$$\overline{G}_\alpha = \frac{A}{\lambda^2} \exp[-(\alpha - 1)^2 \sigma_\ell{}^2] \quad . \qquad (46)$$

It is obvious that this average antenna gain will be maximized when α is chosen to have a value of unit. In this case, the average antenna gain will be equal to the diffraction limited antenna gain given in Eq. (18), i.e., on an average basis there is perfect compensation for the effect of atmospheric turbulence. This perfect compensation is achieved with α equals unity, corresponding exactly to the case of wave function conjugation as the basis for the adaptive optics control. This means that where on the transmitter aperture the intensity of the received signal is low/high the intensity of the transmitted laser beam will be made correspondingly low/high.

1.4 References for Chapter 1

1. R. F. Lutominski and H. T. Yura, "Propagation of a Finite Optical Beam in an Inhomogeneous Medium," Appl. Opt. 10, 1652 (1971).

2. V. I. Tatarski, Wave Propagation in a Turbulent Medium, (McGraw Hill, New York, 1961).

3. D. L. Fried, "Aperture Averaging of Scintillation," J. Opt. Soc. Am. 57, 169 (1967).

4. D. L. Fried, "Optical Resolution Through a Randomly Inhomogeneous Medium for Very Long and Very Short Exposures," J. Opt. Soc. Am. 56, 1372 (1966).

5. V. I. Tatarski, A. S. Gurvich, B. S. Elepov, VI. V. Pokasov, and K. K. Sabelfeld, "Space Structure of Strong Intensity Fluctuations of Light in a Turbulent Medium," Opt. Acta 26, 531 (1979).

Chapter 2

Ambiguity In Image Extraction From Speckle Measurements Using Nonnegativity

2.1 Introduction

It is by now quite well known that nearly diffraction-limited information can be obtained from imagery through turbulence by means of speckle techniques. It was shown by Labeyrie[1] that if a set of very short exposure images is formed, it is possible to determine the power spectrum and correlation function of the diffraction-limited image. The correlation function and the power spectrum are, of course, quite different from the image itself, which is our real interest, but it is possible to learn a great deal about the object and its image from its correlation function, particularly for relatively simple objects like binary stars. However, for more complex objects, there is a pressing need to generate a representation of the image per se, and not just of the correlation function. A rather interesting method of doing this, referred to as the Knox-Thompson algorithm, has been described and analyzed by Knox.[2] However, because of various factors, another approach to this problem has been suggested by Fienup.[3] This approach is based on the still unproven hypothesis that while there are many functions all of which give rise to the same correlation function, the implied ambiguity associated with trying to determine which of the various possible image-functions gave rise to the correlation function measured using Labeyrie's technique can be resolved by noting that the image-function must be everywhere nonnegative. The presumption is that except for a 180°-rotation ambiguity, there is in general only one everywhere nonnegative image-function corresponding to a measured correlation function. It is the purpose of this chapter to explore a certain aspect of this assumption and show under nontrivial conditions that this assumption will break down. Since the conditions we shall consider are far from general in their nature, it is not clear how widely applicable these conditions are. This is a matter we shall leave for the reader to decide.

In the following sections, we shall first develop some mathematical tools, and then in the subsequent section will show how these tools may be used to build up a whole class of image patterns for which there is massive ambiguity in reconstructing the image from the measured correlation function. In the final section, we shall offer some comments and conjectures relating to this result.

2.2 Mathematical Formulation

In the development of this section, we shall draw very heavily upon the mathematical techniques of Bruck and Sodin.[4] We shall assume that without loss of generality, we may consider the image plane to be spatially quantized, and may restrict attention to images of finite extent. We shall consider the spatial quantization to correspond to a square array lattice oriented parallel to the x-y coordinate system axes with lattice spacing Δ, the same along both axes. We shall use the notation (p,q), with p and q both denoting integers, to indicate a particular lattice point. The p,q-lattice point will have coordinates

$$x = p\Delta \quad , \quad y = q\Delta \quad . \tag{1}$$

We shall use the notation $a_{p,q}$ to denote the intensity of some particular image pattern of interest, at the p,q-lattice point. The set of values $\{a_{p,q}\}$ defines the image.

In order for the concept of an image as defined by $\{a_{p,q}\}$ to conform to our practical understanding, it is necessary that we consider two images defined by the coefficients $\{{}_1a_{p,q}\}$ and $\{{}_2a_{p,q}\}$ to be equivalent if for all combinations of values of p and q, we can write any of the following relationships:

For intensity scaling —

$${}_1a_{p,q} = M\,{}_2a_{p,q} \quad , \tag{2}$$

where M is some positive parameter (which does not depend on p and/or q).

For displacement scaling —

$${}_1a_{p,q} = {}_2a_{p-\mu,q-\nu} \quad , \tag{3}$$

where μ and ν are some integer values (which do not depend on p and/or q).

For 180°-rotation scaling

$$ {}_1a_{p,q} = {}_2a_{-p,-q} \quad . \tag{4} $$

Moreover, we will consider the images defined by $\{{}_1a_{p,q}\}$ and by $\{{}_2a_{p,q}\}$ to be equivalent if any sequence of the three transformations defined by Eq.'s (2), (3), and (4) will carry $\{{}_2a_{p,q}\}$ into $\{{}_1a_{p,q}\}$.

The correlation function associated with the image $\{a_{p,q}\}$ is also representable by a set of values on the same square array lattice space. We will use the notation $A_{p,q}$ to denote the correlation value for a displacement of the image with respect to itself equal to $x = p\Delta$ and $y = q\Delta$. Thus we can write

$$ A_{p,q} = \sum_{p',q'} a_{p',q'}\, a_{p'-p,q'-q} \quad . \tag{5} $$

The problem of unambiguous image reconstruction can be viewed as that of trying to determine the values in the set $\{a_{p,q}\}$ thus defining the image, given the set of measured values $\{A_{p,q}\}$ of the correlation function of the image.* It is hoped that any ambiguity inherent in this process can be eliminated by recourse to the constraint that the image is everywhere non-negative, i.e., for all values of p and q , we can write

$$ a_{p,q} \geq 0 \quad . \tag{6} $$

To develop a handle on this question, we shall make use of the ploy of expressing the image by means of a polynomial.

---

* Generally the Labeyrie speckle technique is thought of as providing the power spectrum associated with the image, but can just as well be considered to provide the correlation function.

We shall define the polynomial $f(u, v)$ by the expression

$$f(u, v) = \sum_{p, q} a_{p, q}\, u^p\, v^q \quad . \tag{7}$$

Clearly, a complete knowledge of this polynomial* is entirely equivalent to a knowledge of the image pattern as defined by the set of values $\{a_{p,q}\}$. Not only can the image be defined by a polynomial function, but the correlation function can also be expressed in terms of a polynomial function. The polynomial function

$$F(u, v) = \sum_{p, q} A_{p, q}\, u^p\, v^q \quad , \tag{8}$$

defines the image-correlation function in just the same way that $f(u, v)$ defines the image itself. The problem we are addressing is whether or not (or rather under what conditions) we can unambiguously calculate the polynomial $f(u, v)$ given the polynomial $F(u, v)$.

---

* It is perhaps worth remarking here that Bruck and Sodin[4] arrived at this type of formulation indirectly. They first considered the fourier transformation of the image pattern, which for spatial frequencies κ_x, κ_y can be written as

$$\phi(\kappa_x, \kappa_y) = \sum_{p, q} a_{p, q} \exp\left[-2\pi i (\kappa_x p\Delta + \kappa_y q\Delta)\right] \quad .$$

By defining u and v by the relationships

$$u = \exp(-2\pi i \kappa_x \Delta) \quad , \qquad v = \exp(-2\pi i \kappa_y \Delta) \quad ,$$

they are then able to write

$$\phi(\kappa_x, \kappa_y) = \sum_{p, q} a_{p, q}\, u^p\, v^q$$

and eventually can write

$$f(u, v) = \phi(\kappa_x, \kappa_y) = \sum_{p, q} a_{p, q}\, u^p\, v^q \quad .$$

(Continued on next page)

Making use of Eq.'s (5), (7), and (8), it is now possible to prove a key relationship. Starting with Eq. (7), we can write

$$f(u^{-1}, v^{-1})\, f(u,v) = \left\{ \sum_{P,Q} a_{P,Q}\, u^{-P}\, v^{-Q} \right\} \left\{ \sum_{p \le q'} a_{p \le q'}\, u^{p'}\, v^{q'} \right\}$$

$$= \sum_{\substack{P,Q \\ p \le q'}} a_{p \le q'}\, a_{P,Q}\, u^{p'-P}\, v^{q'-Q} \quad . \tag{9}$$

Now making a change of variables for the summation indices, writing

$$p = p' - P \quad , \qquad q = q' - Q \quad , \tag{10}$$

we can rewrite Eq. (9) as

$$f(u^{-1}, v^{-1})\, f(u,v) = \sum_{\substack{p, q \\ p \le q'}} a_{p \le q'}\, a_{p'-p,\, q'-q}\, u^{p}\, v^{q}$$

$$= \sum_{p,q} \left\{ \sum_{p \le q'} a_{p \le q'}\, a_{p'-p,\, q'-q} \right\} u^{p}\, v^{q} \quad . \tag{11}$$

From Eq. (5), we see that this can be rewritten as

$$f(u^{-1}, v^{-1})\, f(u,v) = \sum_{p,q} A_{p,q}\, u^{p}\, v^{q} \quad . \tag{12}$$

Comparing the right-hand-side of Eq. (12) with Eq. (8), we can see that

$$f(u^{-1}, v^{-1})\, f(u,v) = F(u,v) \quad . \tag{13}$$

---

* (Continued from previous page) This approach makes manifest a relationship between the polynomial $f(u,v)$ and the fourier transform of the image. However, we see no real requirement for this, and therefore have chosen the direct approach of simply writing down Eq. (7) without bringing in fourier transform considerations.

This is a very important mathematical relationship which eventually will show us how to generate all sorts of sample images for which the determination of the image polynomial, $f(u,v)$, from measured values of the image correlation polynomial, $F(u,v)$, is very ambiguous within the nonnegativity constraint of Eq. (6). We shall take this up in the next section.

2.3 Extracting the Image Function From the Correlation Function

The basic problem of processing speckle data as generated by the Labeyrie technique so as to form an estimate of the diffraction-limited image of the object being viewed can be considered equivalent to the following problem. Given the image correlation polynomial function $F(u,v)$ can we find a polynomial function, $f(u,v)$ that has only nonnegative coefficients such that the product $f(u,v)\,f(u^{-1},v^{-1})$ is equal to $F(u,v)$? This problem is presently being studied by Fienup, using an iterative technique.

Implicit in the formulation of this problem is the question of uniqueness, i.e., is there only one such function, $f(u,v)$ for any function $F(u,v)$? In the following, we shall show that the uniqueness criteria is not always satisfied, and in fact will present a technique for generating any desired number of samples of image correlation functions, $F(u,v)$ for which the uniqueness criteria is not satisfied. In judging uniqueness, we of course make allowance for differences in forms of $f(u,v)$ which are "removable" by some combination of the three scaling transformations defined by Eq.'s (2), (3), and (4). Nonetheless, we will be able to show violations of uniqueness.

We shall start by introducing the concept of a "completely factorable" polynomial function. By this we mean a function, $f(u,v)$, which can be written as

$$f(u,v) = \prod_{p,q} (u-\alpha_{p,}) (v-\beta_{q,}) \quad . \tag{14}$$

This is certainly not the most general expression we could write for $f(u,v)$ as there are many choices of the function $f(u,v)$ as defined by Eq. (7) which can not be cast in the form of Eq. (14). For example, such a simple form as $f(u,v)$ equal to $1 + u + v$ is compatible with Eq. (7),

certainly satisfies the nonnegativity constraint of Eq. (6), and is not expressible in the form of Eq. (14). Nonetheless, the set of possible forms of the image function $f(u,v)$ which are compatible with Eq. (14) is extensive, and we have no reason to rule out consideration of such functions, provided that they each satisfy the nonnegativity constraint of Eq. (6). In the following, we shall restrict our attention to image polynomial functions, $f(u,v)$, which are completely factorable, i.e., can be written in a form compatible with Eq. (14).

The zeros of the polynomial $f(u,v)$, i.e., the sets $\{\alpha_{p'}\}$ and $\{\beta_{q'}\}$ define the set of coefficients, $\{a_{p,q}\}$, of the polynomial when expressed in the form of Eq. (7). We could, if we wished, write out the relationships between $a_{p,q}$ and $\{\alpha_{p'}\}$ and $\{\beta_{q'}\}$, but there is no need to do this. It is, however, necessary for us to note that since all of the coefficients $a_{p,q}$ are real, then if any of the zeros, $\alpha_{p'}$ or $\beta_{q'}$, are complex, then their complex conjugate, $\alpha_{p'}^*$ or $\beta_{q'}^*$, must also be a zero. While it is possible for all of the coefficients $a_{p,q}$ to be nonnegative even with zeros, $\alpha_{p'}$ and/or $\beta_{q'}$, which have positive real parts, we are assured that the nonnegativity constraint will be satisfied if all of the zeros have negative real parts. This can be seen by noting that for a real negative zero or a complex conjugate pair of zeros with negative real parts, the corresponding factors will be of the form $(1u + |\alpha_{p'}|)$ or $(1v + |\beta_{q'}|)$ for the real zero, or of the form $(1u^2 + 2u\,|\alpha_{p'}^r| + |\alpha_{p'}|^2)$ or $(1v^2 + 2v \times |\beta_{q'}^r| + |\beta_{q'}|^2)$ for the pair of complex zeros. Here the superscript r, as in $\alpha_{p'}^r$ and $\beta_{q'}^r$, indicate that only the real part of a complex number, $\alpha_{p'}$ or $\beta_{q'}$, respectively, is intended. In each expression, we have written a seemingly superfluous factor of unity for the leading term to make explicit the fact that its coefficient is positive. The important thing to note about these expressions is that as a result of restricting the zeros to the left half plane, we have insured that the corresponding factor in Eq. (14)

contains only positive parameters. This insures that any sum of products of combinations of the parameters in the factors in Eq. (14) will be positive. Since the polynomial coefficients, $a_{p,q}$, in Eq. (7) are each the sum of products of combinations of the parameters in the factors on the right-hand-side of Eq. (14), then we are assured that all of the coefficients, $a_{p,q}$, of the image function polynomial, $f(u,v)$, will satisfy the non-negativity constraint of Eq. (6) if the zeros of the polynomial, $\alpha_{p'}$ and $\beta_{q'}$, are all located in the left half of the complex plane!

We now turn our attention to the zeros of the image correlation function polynomial, $F(u,v)$. We can see from consideration of Eq. (13) that the zeros of $F(u,v)$ will consist of the zeros of $f(u,v)$ plus the zeros of $f(u^{-1},v^{-1})$. The zeros of $f(u^{-1},v^{-1})$ can be determined by noting from Eq. (14) that we can write

$$f(u^{-1},v^{-1}) = \prod_{p',q'} (u^{-1} - \alpha_{p'})(v^{-1} - \beta_{q'}) \quad , \tag{15}$$

from which it follows that the zeros of $f(u^{-1},v^{-1})$ correspond to

$$u^{-1} = \alpha_{p'} \quad , \quad v^{-1} = \beta_{q'} \quad , \tag{16}$$

or

$$u = \alpha_{p'}^{-1} \quad , \quad v = \beta_{q'}^{-1} \quad . \tag{17}$$

The zeros of $f(u^{-1},v^{-1})$ are the sets $\{\alpha_{p'}^{-1}\}$ plus $\{\beta_{q'}^{-1}\}$. Thus the zeros of the image correlation function polynomial, $F(u,v)$, consist of the sets $\{(\alpha_{p'}, \alpha_{p'}^{-1})\}$ plus $\{(\beta_{q'}, \beta_{q'}^{-1}\}$.

The Labeyrie speckle technique, when studying an object whose diffraction-limited image is expressible in the form of Eq. (14), may be considered to yield the image correlation function polynomial, $F(u,v)$, from which we would extract the set of zeros $\{(\alpha_{p'}, \alpha_{p'}^{-1})\}$ plus $\{(\beta_{q'}, \beta_{q'}^{-1})\}$.

Extracting the image function polynomial, $f(u,v)$, from this data corresponds to the task of selecting from each of the P' pairs of zeros, $(\alpha_{p'}, \alpha_{p'}^{-1})$, and the Q' pairs of zeros, $(\beta_{q'}, \beta_{q'}^{-1})$, the correct one of the two zeros in the pair of zeros. There are $2^{P'+Q'}$ possible combinations, all of which will yield an image function polynomial, $f(u,v)$, that is consistent with the measured correlation function, $F(u,v)$, since no matter whether we choose $\alpha_{p'}$ or $\alpha_{p'}^{-1}$ (or $\beta_{q'}$ or $\beta_{q'}^{-1}$), the zeros of the correlation function $F(u,v)$ calculated from that form of $f(u,v)$ will contain both $\alpha_{p'}$ and $\alpha_{p'}^{-1}$ (or $\beta_{q'}$ and $\beta_{q'}^{-1}$), just as does the measured correlation function.

Our sole hope in resolving this $2^{P'+Q'}$ ambiguity lies in the non-negativity constraint of Eq. (6). But unfortunately, if $\alpha_{p'}$ (or $\beta_{q'}$) lies in the left half of the complex plane, then so does $\alpha_{p'}^{-1}$ (or $\beta_{q'}^{-1}$). This is sufficient to insure that whether we correctly choose $\alpha_{p'}$ or incorrectly choose $\alpha_{p'}^{-1}$ (or correctly choose $\beta_{q'}$ or incorrectly choose $\beta_{q'}^{-1}$) the non-negativity constraint will be satisfied! Seemingly, then, if we consider an image function, $f(u,v)$, which is completely factorable in the sense of Eq. (14), and if all of the zeros of this function lie in the negative half of the complex plane, then there is an unavoidable ambiguity in the process of trying to extract the image function, $f(u,v)$ from the measured image correlation function, $F(u,v)$!

The ambiguity will be of the order of $2^{P'+Q'}-2$, the minus two being there since one set of choices, namely $\{\alpha_{p'}\}$ plus $\{\beta_{q'}\}$ will be strictly correct, while the choice of all of the inverse zeros, i.e. $\{\alpha_{p'}^{-1}\}$ plus $\{\beta_{q'}^{-1}\}$ will be equivalent to the correct choice on the basis of the 180° rotation scaling law of Eq. (4). But $2^{P'+Q'}-2$ is a large degree of ambiguity. Thus we see that at least for one class of objects, namely, those corresponding to image function polynomials which are completely factorable and having all of their zeros in the left half of the complex plane, the ambiguity associated with the process of extracting the image from speckle data of the type generated by the Labeyrie technique will be very large.

2.4 Comments and Conclusions

The set of images for which the image function polynomial is completely factorable with all of its zeros in the left half of the complex plane is certainly much less than the set of all possible images. Nonetheless, since there is no reason to believe that these are basically uninteresting images, we are forced to conclude that we can not, in general, extract an image from its power spectrum or correlation function with the aid of the nonnegativity constraint. Accordingly, we conclude that speckle data for image development should preferably be processed by a technique which relies on something like the Knox-Thompson algorithm[2] to develop all of the details of the image directly (and analytically) from the speckle data, rather than attempting to process the speckle data by means of the Labeyrie technique in conjunction with the nonnegativity constraint. We believe it would prove interesting to generate several completely factorable images, with left half plane zeros, and attempt their reconstruction from speckle data processed using the Labeyrie technique.

2.5 References for Chapter 2

1. A. Labeyrie, "Attainment of Diffraction Limited Resolution in Large Telescopes by Fourier Analyzing Speckle Patterns in Star Images," Astr. and Ap. 6, 85 (1970).

2. K. T. Knox, Diffraction-Limited Imaging With Astronomical Telescopes, PhD Thesis, Institute of Optics, the University of Rochester, Rochester, N.Y. 1975

3. J. R. Fienup, "Reconstruction Of An Object From The Modulus Of Its Fourier Transform," Opt. Lett. 3, 27 (1978)

4. Yu. M. Bruck and L. G. Sodin, "On The Ambiguity Of The Image Reconstruction Problem," Opt. Comm. 30, 304 (1979)

Chapter 3

Electrically Induced Mirror Deflections:

An Improved Method

3.1 Problem Formulation and Basic Approach

The performance of optical systems employing large diameter optical elements is degraded by distortions of the wavefront induced by atmospheric instabilities. One method which has been employed to reduce this degradation is to deform a mirror used as part of the optical system in such a manner as to compensate for the wavefront distortion caused by the atmosphere. In the Compensated Imaging System, this has been implemented by bonding a relatively thin glass mirror to a piezoelectric disk and applying an electric field across the disk's thickness with an appropriate spatial distribution of field strength over the face of the disk, so as to produce the desired compensating distortion of the disk's thickness and thus of the mirror bonded to the disk.

The currently established procedure is to use a piezoelectric ceramic substrate polarized normal to the surface to which the deformable mirror is bonded, and apply an electric field parallel to the direction of polarization. One surface of the piezoelectric substrate is covered with a continuous electrode, and the other, which lies just below the mirror, is covered with a mosaic of electrically isolated electrodes. By applying differing voltages to the various electrodes in the mosaic, the desired spatially varying field can be produced. At least nominally, the voltage required to produce a given change, ΔT , in thickness of the piezoelectric substrate is given by

$$\Delta T = d_{33} V \quad , \tag{1}$$

where d_{33} is the constant relating strain along the polarization axis to field strength parallel to the same axis.

The chief problem with this approach is the large voltages (typically, well in excess of 1000 volts) required to produce the desired mirror surface deflections. It is to be noted that the required voltage is independent

of the thickness of the ceramic substrate, so no reduction in driving voltage can be achieved by varying this parameter. It is possible, however, to greatly reduce the required driving voltage through use of a fundamentally different type of piezoelectric configuration. It is possible to reduce the required voltage by taking advantage of the d_{31} constant of the piezoelectric ceramic. This is achieved by applying the electric field parallel to the polarization axis as before, but utilizing the deflection along an axis normal to the polarization axis to deform the mirror. It is this concept which we wish to develop into a reasonable configuration and then evaluate its performance.

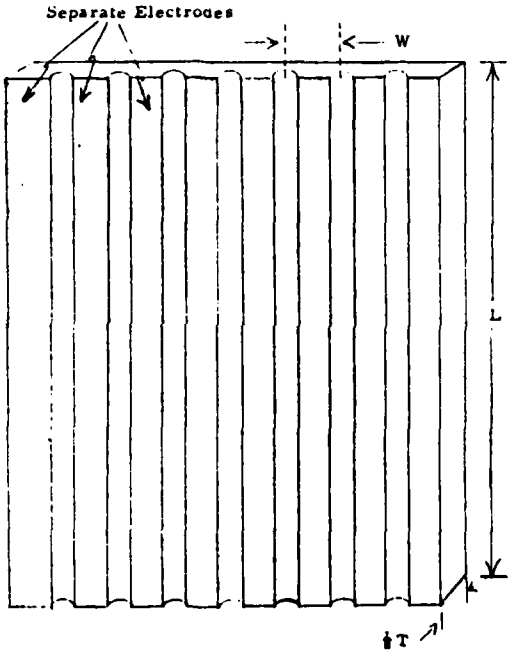

Figure 1. Single Sheet Unit with Multiple d_{31} Piezoelectric Elements.

Consider a sheet of piezoelectric material as shown in Fig. 1. If the back of the slab is covered with a continuous electrode and a voltage is applied between it and one of the front electrodes, the deflection along the L direction will be approximately

$$\Delta L = 2\ V\ d_{31}\ L/T \quad . \qquad (2)$$

For this configuration, the deflection for a given voltage is proportional to L/T . The voltage required to achieve a desired distortion can be reduced by a suitable choice of the element dimensions.

If these slabs are cemented together into a set, as shown in Fig. 2, with alternating facing of the slabs (i.e., slotted sides to slotted sides, and unslotted sides to unslotted sides), and the ratio of L to T is made large, the resulting composite could be used as a substrate to produce some required deformation of a mirror with a much lower voltage than is needed to produce that deflection when the substrate utilizes the d_{33} piezoelectric constant. However, this analysis is overly simplistic in that when the ratio of L to T is large, and W is made equal to T (required for elements of square cross section), then there is a very strong mechanical coupling between neighboring elements, so that the deflection of an element whose neighbors are not deflected is substantially less than indicated by Eq. (2). A quantitative analysis of the effect of this undesired coupling of adjacent elements will be found in the Appendix.

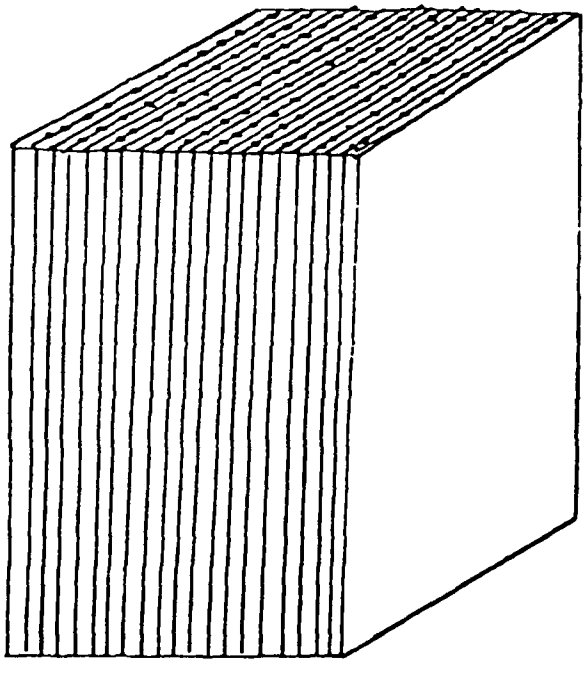

Figure 2. Multiple Sheet Unit with Two-Dimensional Array of d_{31} Piezoelectric Elements.

3.2 Approach Refinement

To avoid this limitation, the elements must be mechanically decoupled. Since the shear modulus determines the mechanical coupling, one possibility would be to cut the elements completely apart and then bond them together with a thin layer of some material, such as indium, whose shear modulus is low in comparison to that of the piezoelectric ceramic, in the hope that this would provide sufficient decoupling. Unfortunately, the shear modulus of piezoelectric ceramics with a large d_{31} constant (e.g., EC-70) is only about ten times that of indium. Thus, although some decoupling can be accomplished with this technique, it is not sufficient to permit the use of large values of L/T, with the implication of very low values of required voltage.

A more satisfactory approach is to cut the elements apart and then mechanically hold them together in an array without actually bonding them. This can be realized based on the following procedure. A thin copper foil electrode, as shown in Fig. 3, is sandwiched between two piezoelectric ceramic slabs. The total thickness, T , of the resulting sandwich will be twice that of a slab. A set of narrow slots are then cut into the sandwich starting from each end to near the middle to separate the individual elements, as shown in Fig. 4. The slots extend sufficiently close to the middle so as to reach the preslotted part of the copper foil, resulting in electrical isolation of copper foil strips. (The slots may be filled with a potting compound to provide a measure of mechanical stability for the elements.) The array is then built by stacking a number of these piezoelectric/copper sandwiches alternately with thin sheets of steel lubricated by graphic or some other solid lubricant. The entire array is held together by a clamp around its central band which applies force normal to the plane of the steel separator plates,

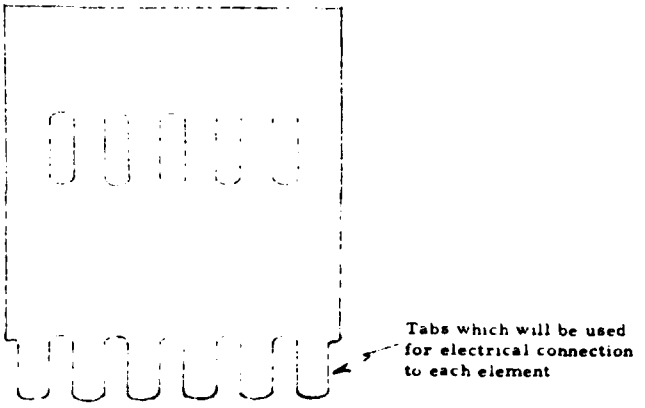

Figure 3. Copper Foil Electrodes Initial Pattern.

Copper electrode before slots are cut in the ceramic slab.

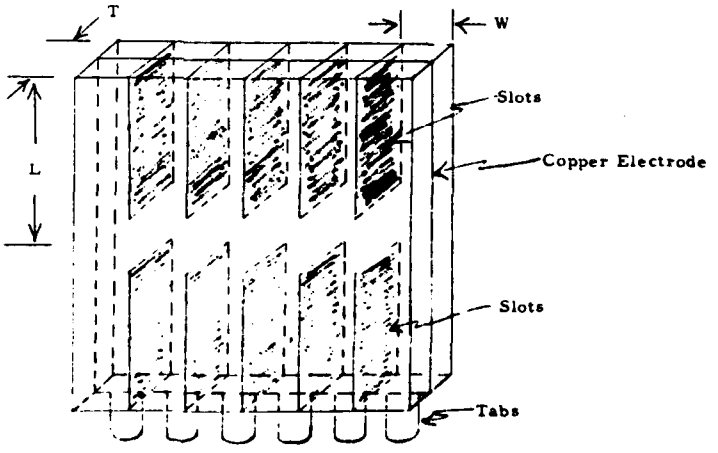

Figure 4. Piezoelectric/Copper Foil Sandwich.

Ceramic slabs show slots cut to separate elements. The portion of the elements in the lower half are used to provide a reaction to the motion of the elements in the upper half.

near the middle. These clamps extend only over the unslotted middle part of the array, as shown in Fig. 5.

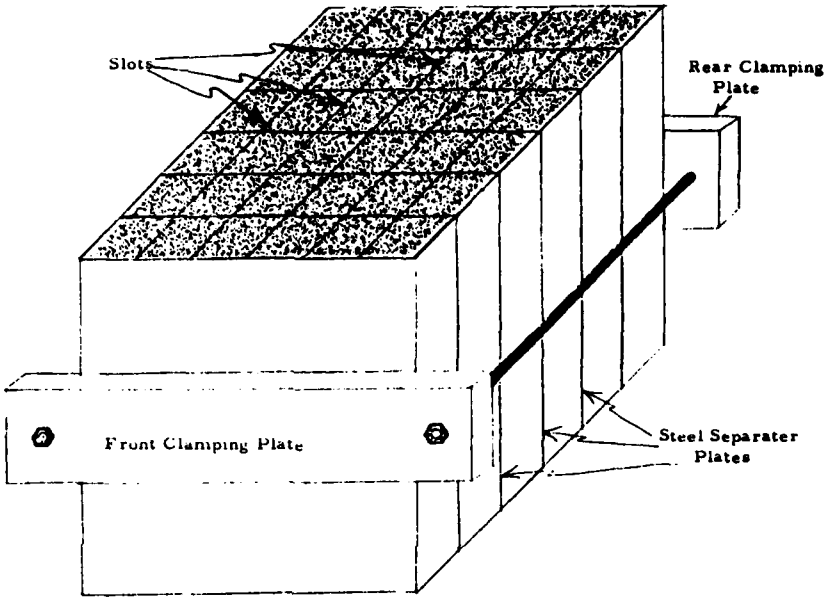

Figure 5. Two-Dimensional Array of d_{31} Piezoelectric Elements.
The gray shaded area is the top of the array and will be covered by a deformable thin glass mirror.

The individual copper electrodes serve to activate individual piezoelectric elements, and the steel separator plates serve as a common electrode. The deflection of the elements will be given by

$$\Delta L = 2\ V\ d_{31}\ \ L/T \quad , \tag{3}$$

since the separation of the electrodes is $T/2$. This assumes that the unit is mounted at the center so that the displacement of the lower half of each element provides only a compensating reaction, and produces no useful displacement.

3.3 Friction Considerations

The frictional forces between the electrodes and the steel plates will produce a small hysteresis type effect in the electrode motion, which can be calculated as follows: Assume that the clamping pressure is P, and that the coefficient of friction between the ceramic and steel is C. The friction force opposing the motion of an element will be $PCW\ell$ distributed over the length of the element. Here ℓ denotes the L direction dimension of the clamp. It is only over this range, ℓ, that the friction force is significant. This will reduce the electrode motion by

$$R = \frac{PC\ell^2}{2\,T\,E_\ell} \quad , \tag{4}$$

where E_ℓ is the longitudinal modulus of elasticity of the piezoelectric ceramic. Using Eq. (3) to determine the "friction voltage" required to compensate for this reduction, we get

$$V_f = \frac{PC\ell^2/L}{4\,E_\ell\,d_{31}} \quad . \tag{5}$$

For example, if

$$P = 6.9 \times 10^4 \text{ N/M}^2 \equiv (10 \text{ psi})$$
$$C = 0.05$$
$$\ell = 0.01 \text{ m}$$
$$L = 0.1 \text{ m}$$

and assuming that the piezoelectric is EC-70, for which

$$E_\ell = 6.4 \times 10^{10} \text{ N/M}^2$$
$$d_{31} = 225 \times 10^{-12} \text{ V/M} \quad ,$$

then $V_f = 0.06$ volts. This represents the hysteresis voltage, the additional voltage [in excess of that specified by Eq. (3)] that must be applied to the elements to overcome the frictional forces.

It is to be noted that this value of the "friction voltage" does not depend on T. It can be seen that an attempt to reduce the required voltage to achieve the desired mirror distortion by reducing T can result in a significant hysteresis problem when the invariant value of the "friction voltage" becomes a significant factor compared to the driving voltage. The minimum useful value of T will be determined by the requirement that the "friction voltage," which will appear as though produced by a hysteresis effect, contribute no more than some specified displacement. Making use of Eq. (3) and allowing no more than some small displacement, ΔL, due to the friction voltage, the allowed limit on thickness T will be

$$T \geq 2 V_F d_{31} L/\Delta L_F \quad . \tag{6}$$

If we are willing to allow on a displacement

$$\Delta L_F = 2.5 \times 10^{-8} \text{ m} \quad , \quad (\text{i.e., } \lambda/20 \text{ @ } \lambda = 5 \times 10^{-7} \text{ m})$$

then with the parameters given above, we find from Eq. (6) that

$$T \geq 1.08 \times 10^{-4} \text{ m} \quad .$$

This constraint is so small as to be of no particular significance.

Thus far no mention has been made of the coupling between elements due to the potting compound. It will not be significant as long as the shear modulus of the compound multiplied by the ratio of the slot length to the slot width is small compared to the shear modulus of the piezoelectric ceramic. If this is not the case, the potting compound can be replaced by some nonconducting solid strips (e.g., teflon) which will just fill the slots and thereby prevent lateral motion of the ceramic elements. This may be desirable in any event, since it will eliminate any tendency for the elements to buckle even if they are very long and thin. A very soft potting compound might not provide enough mechanical stability.

3.4 General Considerations

When the completed array is being ground and polished in preparation for bonding the mirror to its front face, it probably will be desirable to apply clamping not only near the center, as shown in Fig. 5, but also near the top of the array, and to increase the clamping force beyond the 10 psi used in the examples. This, along with keeping the motion of the polisher normal to the plane of the steel separator plates, will insure that the ends of the elements are not bent or broken by the polishing action. When the polishing is complete, the clamp near the top would be removed, and at the middle the clamping pressure would be reduced to 10 psi to reduce the frictional forces.

The following considerations should be borne in mind when selecting the element length, L. If L is large, the resonant frequency of the element will be reduced, thus reducing the upper limit of the operational frequency of the array. ($L = 10$ cm implies a resonant frequency of about 10,000 Hz.) If L is small, T will also have to be small to get the required displacements from the driving voltage [cf. Eq. (3)]. Also, as T decreases, the ratio of active area (piezoelectric ceramic) to total area (including inactive components — steel separator plates, copper electrodes, and slots) decreases. If this ratio gets too small (less than $\frac{1}{2}$), there may be insufficient coupling between the array and the mirror. The relative importance of all these factors will have to be assessed in more detail to determine the best value of L. Properly chosen values of L and T will produce an array capable of deforming the attached mirror with a voltage far less than is required by current piezoelectric ceramic substrates utilizing the d_{33} constant.

Appendix to Chapter 3

If a voltage, V, is applied to just one element of width, W, in the configuration shown in Fig. 1, its deflection will be reduced somewhat by the neighboring elements which, of course, are physically attached to it, but are not being deflected electrically. The magnitude of the reduction will depend on the ratio of W to L. If W is very large, the effect of the adjoining elements will be felt only in the neighborhood of the boundaries. The deflection at the center of the element will be almost unaffected. As W gets smaller, eventually the motion of even the center of the element will be affected. The value at which this occurs represents W_{MIN}, the minimum value for W for which the approximate deflections given by Eq. (2) are applicable.

W_{MIN} may be evaluated as follows: Fig. 6 shows a single element being deflected electrically when $W \cong W_{MIN}$. In particular, consider a small section dX of the element being activated, located at a distance X from the base of the element. When the field is applied to dX inducing a strain, ϵ_E, the section will increase in length by $\epsilon_E\, dX$. This will induce a shear strain of $\frac{\epsilon_E\, dX}{W}$ in the material above dX. This shear strain induces a shear stress which tends to compress the portion of the element below dX. The shear force is $2(L-X)\, T \frac{\epsilon_E\, dX}{W} E_s$, where E_s is the shear modulus of elasticity, and the factor of 2 is due to there being two neighboring undeflected elements. The factor $(L-X)\, T$ is the cross sectional area along the shear plane of the material above dX. The compression (of the element below dX) caused by this force is given by

$$C_1 = \frac{2\,(L-X)\,\epsilon_E\, dX\, E_s\, X}{W^2\, E_\ell} \quad , \tag{A1}$$

where E_ℓ is the longitudinal modulus of elasticity of the material.

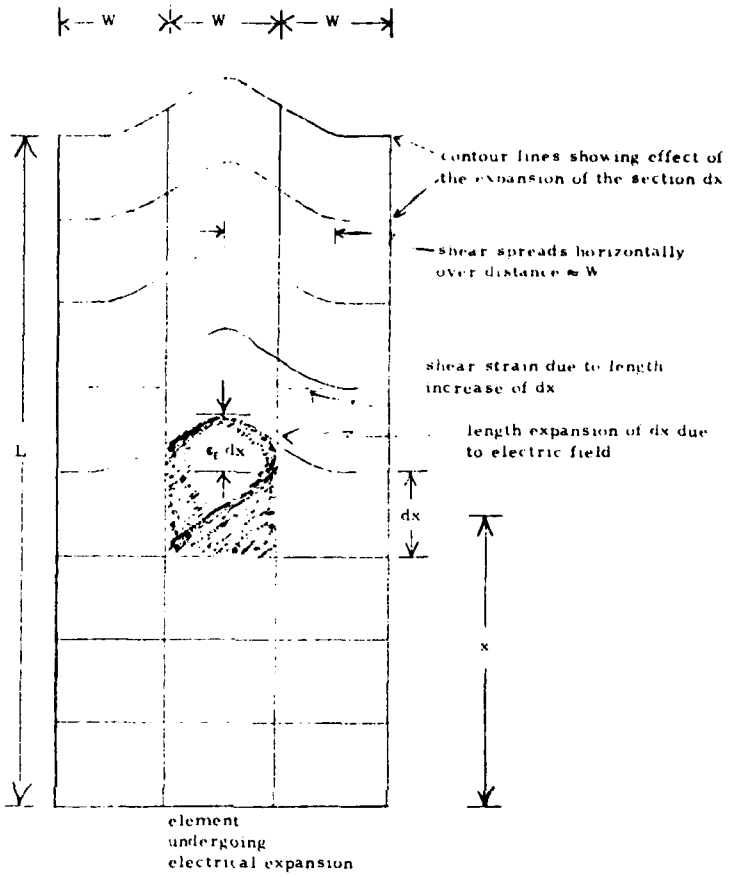

Figure 6. Single Element Piezoelectric Action as Constrained by Neighboring Elements.

Additionally, the material above dX will be compressed by the shear forces, the exact amount varying according to its location. Consider a small section, dY , located at a distance Y from the section, dX , as shown in Fig. 7. It will be subjected to a compressional force, F_2 , given by

$$F_2 = 2\,(L-X-Y)\,T\,\frac{\epsilon_t\,dX}{W}\,E_s \quad . \tag{A2}$$

This, in turn, will cause a compression of dY , given by

$$d\,C_2 = \frac{2\,(L-X-Y)\,\epsilon_t\,dX\,E_s\,dY}{W^2\,E_\ell} \quad , \tag{A3}$$

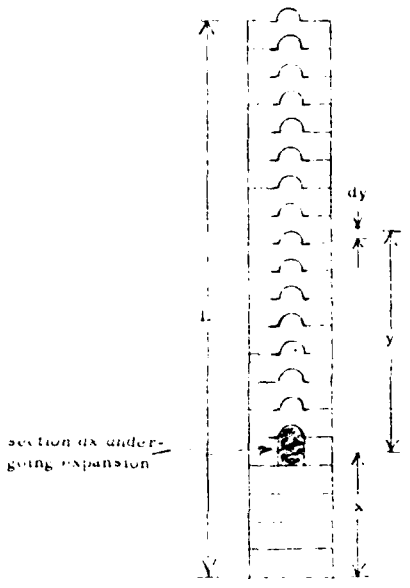

Figure 7. Single Element Piezoelectric Displacement.

The total compression of the material above dX is thus

$$C_2 = \frac{2\ e_t\ dX\ E_s}{W^2\ E_\ell} \int_0^{L-x} (L-X-Y)\ dY \quad , \tag{A4}$$

$$C_2 = \frac{2\ e_t\ dX\ E_s}{W^2\ E_\ell} \left[\frac{L^2}{2} - LX + \frac{X^2}{2}\right] \quad , \tag{A5}$$

and the total compression of the whole element due to the shear forces induced by the expansion of dX is

$$C_1 + C_2 = \frac{2\ e_t\ E_s}{W^2\ E_\ell} \left[\frac{L^2}{2} - \frac{X^2}{2}\right] dX \quad . \tag{A6}$$

A measure of the degree to which this compression reduces the electrical expansion of dX is given by

$$E_{dx} = \frac{2\ e_t\ dX - (C_1 + C_2)}{e_t\ dX} \quad , \tag{A7}$$

where it will be remembered $\epsilon_E\, dX$ is the electrical expansion of dX. Substituting the value of $C_1 + C_2$, we get

$$E_{dX} = 1 - \frac{2\, E_s}{W^2\, E_\ell} \left(\frac{L^2}{2} - \frac{X^2}{2} \right) \quad . \tag{A8}$$

The ratio, E, for the entire element is

$$E = \frac{\int_0^L E_{dX}\, dX}{L} \quad , \tag{A9}$$

or

$$E = 1 - \frac{2}{3} \frac{E_s}{E_\ell} \frac{L^2}{W^2} \quad . \tag{A10}$$

It should be noted that two approximations have been made in this analysis. Since the shear stresses tend to compress the element which is expanding, the final shear strains will be somewhat less than used here, but for values of E close to 1, the error (an underestimation) will not be large. This analysis also assumes that the expansion of dX induces shear stresses only in the material above dX. Since there is no discontinuity at dX, some shear stress must propagate below dX as well. An approximation ignoring shear stress below dX tends to overestimate E. Eq. (A10) does, however, yield an insight into the effect of the ratio of L to W on the behavior of E. Taking the ratio E_s/E_ℓ to be 1/3 for the piezoelectric ceramic, and requiring that E be $\geq \frac{1}{2}$, we find

$$\frac{L^2}{W^2} \leq \frac{9}{4} \quad , \quad \text{or} \tag{A11}$$

$$W \geq \tfrac{2}{3} L \quad (\text{i.e.,} \quad W_{MIN} = \tfrac{2}{3} L) \quad . \tag{A12}$$

If W is significantly smaller than this, E quickly gets very small due to the quadratic dependence on the L/W ratio. E, of course, can never be less than zero. Of course, Eq. (A10) becomes less and less accurate as E deviates from 1.

If the cross section of the elements is made rectangular with $W \cong L$ and $T \ll L$, then large deflections as predicted by Eq. (2) can be realized. If, however, it is required that $W = T$, then either L/T will not be much larger than 1, or E will be very small. In either case, the use of the d_{31} mode will not give an appreciable improvement over the more conventional d_{33} mode for this configuration. Decoupling between the elements, as suggested in Fig.'s 4 and 5, is required to avoid this severe limitation.